

Moments of the Spin Structure Functions g_1^p and g_1^d for $0.05 < Q^2 < 3.0 \text{ GeV}^2$

Y. Prok,⁸ P. Bosted,³⁵ V.D. Burkert,³⁵ A. Deur,³⁵ K.V. Dharmawardane,²⁹ G.E. Dodge,^{29,*} K.A. Griffioen,³⁹ S.E. Kuhn,²⁹ R. Minehart,³⁸ G. Adams,³¹ M.J. Amarian,²⁹ M. Anghinolfi,¹⁸ G. Asryan,⁴⁰ G. Audit,⁷ H. Avakian,^{17,35} H. Bagdasaryan,^{40,29} N. Baillie,³⁹ J.P. Ball,² N.A. Baltzell,³⁴ S. Barrow,¹³ M. Battaglieri,¹⁸ K. Beard,²¹ I. Bedlinskiy,²⁰ M. Bektasoglu,²⁹ M. Bellis,⁵ N. Benmouna,¹⁴ B.L. Berman,¹⁴ A.S. Biselli,^{31,11} L. Blaszczak,¹³ S. Boiarinov,^{20,35} B.E. Bonner,³² S. Bouchigny,^{35,19} R. Bradford,⁵ D. Branford,¹⁰ W.J. Briscoe,¹⁴ W.K. Brooks,³⁵ S. Bültmann,²⁹ C. Butuceanu,³⁹ J.R. Calarco,²⁶ S.L. Careccia,²⁹ D.S. Carman,³⁵ L. Casey,⁶ A. Cazes,³⁴ S. Chen,¹³ L. Cheng,⁶ P.L. Cole,^{35,16} P. Collins,² P. Coltharp,¹³ D. Cords,^{35,†} P. Corvisiero,¹⁸ D. Crabb,³⁸ V. Crede,¹³ J.P. Cummings,³¹ D. Dale,¹⁶ N. Dashyan,⁴⁰ R. De Masi,⁷ R. De Vita,¹⁸ E. De Sanctis,¹⁷ P.V. Degtyarenko,³⁵ H. Denizli,³⁰ L. Dennis,¹³ K.S. Dhuga,¹⁴ R. Dickson,⁵ C. Djalali,³⁴ D. Doughty,^{8,35} M. Dugger,² S. Dytmann,³⁰ O.P. Dzyubak,³⁴ H. Egiyan,^{39,35} K.S. Egiyan,^{40,†} L. El Fassi,¹ L. Elouadrhiri,^{8,35} P. Eugenio,¹³ R. Fatemi,³⁸ G. Fedotov,²⁵ G. Feldman,¹⁴ R.G. Fersh,³⁹ R.J. Feuerbach,³⁹ T.A. Forest,^{29,16} A. Fradi,¹⁹ H. Funsten,^{39,†} M. Garçon,⁷ G. Gavalian,^{26,29} N. Gevorgyan,⁴⁰ G.P. Gilfoyle,³³ K.L. Giovanetti,²¹ F.X. Girod,⁷ J.T. Goetz,³ E. Golovatch,¹⁸ R.W. Gothe,³⁴ M. Guidal,¹⁹ M. Guillo,³⁴ N. Guler,²⁹ L. Guo,³⁵ V. Gyurjyan,³⁵ C. Hadjidakis,¹⁹ K. Hafidi,¹ H. Hakobyan,⁴⁰ C. Hanretty,¹³ J. Hardie,^{8,35} N. Hassall,¹⁵ D. Heddle,³⁵ F.W. Hersman,²⁶ K. Hicks,²⁸ I. Hleiqawi,²⁸ M. Holtrop,²⁶ M. Huertas,³⁴ C.E. Hyde-Wright,²⁹ Y. Ilieva,¹⁴ D.G. Ireland,¹⁵ B.S. Ishkhanov,²⁵ E.L. Isupov,²⁵ M.M. Ito,³⁵ D. Jenkins,³⁷ H.S. Jo,¹⁹ J.R. Johnstone,¹⁵ K. Joo,^{35,9} H.G. Juengst,²⁹ N. Kalantarians,²⁹ C.D. Keith,³⁵ J.D. Kellie,¹⁵ M. Khandaker,²⁷ K.Y. Kim,³⁰ K. Kim,²² W. Kim,²² A. Klein,²⁹ F.J. Klein,^{12,6} M. Klusman,³¹ M. Kossov,²⁰ Z. Krahm,⁵ L.H. Kramer,^{12,35} V. Kubarovskiy,^{31,35} J. Kuhn,^{31,5} S.V. Kuleshov,²⁰ V. Kuznetsov,²² J. Lachniet,^{5,29} J.M. Laget,^{7,35} J. Langheinrich,³⁴ D. Lawrence,²⁴ Ji Li,³¹ A.C.S. Lima,¹⁴ K. Livingston,¹⁵ H.Y. Lu,³⁴ K. Lukashin,⁶ M. MacCormick,¹⁹ C. Marchand,⁷ N. Markov,⁹ P. Mattione,³² S. McAleer,¹³ B. McKinnon,¹⁵ J.W.C. McNabb,⁵ B.A. Mecking,³⁵ M.D. Mestayer,³⁵ C.A. Meyer,⁵ T. Mibe,²⁸ K. Mikhailov,²⁰ M. Mirazita,¹⁷ R. Miskimen,²⁴ V. Mokeev,^{25,35} L. Morand,⁷ B. Moreno,¹⁹ K. Moriya,⁵ S.A. Morrow,^{19,7} M. Moteabbed,¹² J. Mueller,³⁰ E. Munevar,¹⁴ G.S. Mutchler,³² P. Nadel-Turonski,¹⁴ R. Nasseripour,^{12,34} S. Niccolai,^{14,19} G. Niculescu,^{28,21} I. Niculescu,^{14,21} B.B. Niczyporuk,³⁵ M.R. Niroula,²⁹ R.A. Niyazov,^{29,35} M. Nozar,³⁵ G.V. O'Rielly,¹⁴ M. Osipenko,^{18,25} A.I. Ostrovidov,¹³ K. Park,²² E. Pasyuk,² C. Paterson,¹⁵ S. Anefalos Pereira,¹⁷ S.A. Philips,¹⁴ J. Pierce,³⁸ N. Pivnyuk,²⁰ D. Pocanic,³⁸ O. Pogorelko,²⁰ I. Popa,¹⁴ S. Pozdniakov,²⁰ B.M. Preedom,³⁴ J.W. Price,⁴ S. Procureur,⁷ D. Protopopescu,^{26,15} L.M. Qin,²⁹ B.A. Raue,^{12,35} G. Riccardi,¹³ G. Ricco,¹⁸ M. Ripani,¹⁸ B.G. Ritchie,² G. Rosner,¹⁵ P. Rossi,¹⁷ D. Rowntree,²³ P.D. Rubin,³³ F. Sabatié,^{29,7} J. Salamanca,¹⁶ C. Salgado,²⁷ J.P. Santoro,^{37,6,35} V. Sapunenko,^{18,35} R.A. Schumacher,⁵ M.L. Seely,³⁵ V.S. Serov,²⁰ Y.G. Sharabian,³⁵ D. Sharov,²⁵ J. Shaw,²⁴ N.V. Shvedunov,²⁵ A.V. Skabelin,²³ E.S. Smith,³⁵ L.C. Smith,³⁸ D.I. Sober,⁶ D. Sokhan,¹⁰ A. Stavinsky,²⁰ S.S. Stepanyan,²² S. Stepanyan,^{35,8,40} B.E. Stokes,¹³ P. Stoler,³¹ I.I. Strakovsky,¹⁴ S. Strauch,³⁴ R. Suleiman,²³ M. Taiuti,¹⁸ D.J. Tedeschi,³⁴ A. Tkabladze,¹⁴ S. Tkachenko,²⁹ L. Todor,⁵ M. Ungaro,^{31,9} M.F. Vineyard,^{36,33} A.V. Vlassov,²⁰ D.P. Watts,¹⁰ L.B. Weinstein,²⁹ D.P. Weygand,³⁵ M. Williams,⁵ E. Wolin,³⁵ M.H. Wood,³⁴ A. Yegneswaran,³⁵ J. Yun,²⁹ L. Zana,²⁶ J. Zhang,²⁹ B. Zhao,⁹ and Z.W. Zhao³⁴

(The CLAS Collaboration)

¹Argonne National Laboratory

²Arizona State University, Tempe, Arizona 85287-1504

³University of California at Los Angeles, Los Angeles, California 90095-1547

⁴California State University, Dominguez Hills, Carson, CA 90747

⁵Carnegie Mellon University, Pittsburgh, Pennsylvania 15213

⁶Catholic University of America, Washington, D.C. 20064

⁷CEA-Saclay, Service de Physique Nucléaire, 91191 Gif-sur-Yvette, France

⁸Christopher Newport University, Newport News, Virginia 23606

⁹University of Connecticut, Storrs, Connecticut 06269

¹⁰Edinburgh University, Edinburgh EH9 3JZ, United Kingdom

¹¹Fairfield University, Fairfield CT 06824

¹²Florida International University, Miami, Florida 33199

¹³Florida State University, Tallahassee, Florida 32306

¹⁴The George Washington University, Washington, DC 20052

¹⁵University of Glasgow, Glasgow G12 8QQ, United Kingdom

¹⁶Idaho State University, Pocatello, Idaho 83209

- ¹⁷INFN, Laboratori Nazionali di Frascati, 00044 Frascati, Italy
¹⁸INFN, Sezione di Genova, 16146 Genova, Italy
¹⁹Institut de Physique Nucleaire ORSAY, Orsay, France
²⁰Institute of Theoretical and Experimental Physics, Moscow, 117259, Russia
²¹James Madison University, Harrisonburg, Virginia 22807
²²Kyungpook National University, Daegu 702-701, South Korea
²³Massachusetts Institute of Technology, Cambridge, Massachusetts 02139-4307
²⁴University of Massachusetts, Amherst, Massachusetts 01003
²⁵Moscow State University, General Nuclear Physics Institute, 119899 Moscow, Russia
²⁶University of New Hampshire, Durham, New Hampshire 03824-3568
²⁷Norfolk State University, Norfolk, Virginia 23504
²⁸Ohio University, Athens, Ohio 45701
²⁹Old Dominion University, Norfolk, Virginia 23529
³⁰University of Pittsburgh, Pittsburgh, Pennsylvania 15260
³¹Rensselaer Polytechnic Institute, Troy, New York 12180-3590
³²Rice University, Houston, Texas 77005-1892
³³University of Richmond, Richmond, Virginia 23173
³⁴University of South Carolina, Columbia, South Carolina 29208
³⁵Thomas Jefferson National Accelerator Facility, Newport News, Virginia 23606
³⁶Union College, Schenectady, NY 12308
³⁷Virginia Polytechnic Institute and State University, Blacksburg, Virginia 24061-0435
³⁸University of Virginia, Charlottesville, Virginia 22901
³⁹College of William and Mary, Williamsburg, Virginia 23187-8795
⁴⁰Yerevan Physics Institute, 375036 Yerevan, Armenia
- (Dated: February 6, 2020)

The spin structure functions g_1 for the proton and the deuteron have been measured over a wide kinematic range in x and Q^2 using 1.6 and 5.7 GeV longitudinally polarized electrons incident upon polarized NH_3 and ND_3 targets at Jefferson Lab. Scattered electrons were detected in the CEBAF Large Acceptance Spectrometer, for $0.05 < Q^2 < 5 \text{ GeV}^2$ and $W < 3 \text{ GeV}$. The first moments of g_1 for the proton and deuteron are presented – both have a negative slope at low Q^2 , as predicted by the extended Gerasimov-Drell-Hearn sum rule. The first result for the generalized forward spin polarizability of the proton γ_0^p is also reported. This quantity shows strong Q^2 dependence at low Q^2 , while $Q^6\gamma_0^p$ seems to flatten out at the highest Q^2 accessed by our experiment. Although the first moments of g_1 are consistent with Chiral Perturbation Theory (χPT) calculations up to approximately $Q^2 = 0.06 \text{ GeV}^2$, a significant discrepancy is observed between the γ_0^p data and χPT for γ_0^p , even at the lowest Q^2 .

PACS numbers: 13.60.Hb;13.88.+e;14.20.Dh

Keywords: Spin structure functions, nucleon structure, Chiral Perturbation Theory

Fundamental to our understanding of nuclear matter is a complete picture of the spin structure of the nucleon. The spin of the nucleon arises from the spin and orbital angular momenta of both the quarks and gluons. One way to access the quark spins in lepton scattering is through measurements of the spin structure functions g_1 and g_2 [1], which are not well known at low momentum transfer to the target nucleon ($Q^2 < 2 \text{ GeV}^2$). At larger momentum transfer, $g_1(x, Q^2) = \frac{1}{2}\sum e_i^2\Delta q_i(x)$ (in the parton picture), where $\Delta q_i/q_i$ is the net helicity of quarks of flavor i in the direction of the (longitudinally polarized) nucleon spin, q_i is the probability of finding a quark of flavor i with momentum fraction x , and e_i is the quark charge. (The Bjorken scaling variable $x = \frac{Q^2}{2M\nu}$ in the lab frame, M is the nucleon mass and ν is the energy transferred from the electron to the target nucleon.) At sufficiently small Q^2 , g_1 and its moments can be more economically described by hadronic degrees of freedom and effective low-energy approximations to QCD, like

Chiral Perturbation Theory (χPT).

There is particular interest in the first moment of g_1 , $\Gamma_1(Q^2) = \int_0^{x_0} g_1(x, Q^2)dx$, which is related to the fraction of the nucleon spin carried by quark spins. The upper limit of the integral, x_0 , corresponds to pion production threshold. This limit excludes elastic scattering, which otherwise dominates the low Q^2 behavior of the integral. Γ_1 is constrained as $Q^2 \rightarrow 0$ by the Gerasimov-Drell-Hearn (GDH) sum rule [2, 3] to be $-\frac{\kappa^2}{8M^2}Q^2$, where κ is the anomalous magnetic moment of the nucleon. At high Q^2 , Γ_1 has been measured in deep inelastic scattering (DIS) experiments at SLAC [4, 5], CERN [6, 7, 8] and DESY [9]. Ji and Osborne [10] have shown that the GDH sum rule can be generalized to all Q^2 via

$$\Gamma_1(Q^2) = \frac{Q^2}{8}S_1(\nu = 0, Q^2) - \Gamma_1^{el}(Q^2), \quad (1)$$

where $S_1(\nu, Q^2)$ is the spin-dependent virtual photon Compton amplitude and Γ_1^{el} is the contribution to the integral from elastic scattering. At high Q^2 , S_1 can be

calculated using the operator product expansion (OPE). By comparing the OPE twist series with Γ_1 , one can extract higher twist parameters [11, 12, 13, 14, 15], which are sensitive to quark-gluon and quark-quark correlations in the nucleon at moderate Q^2 . Lattice QCD calculations may eventually be available in the moderate Q^2 region below the range of applicability of the OPE. At low Q^2 , S_1 can be calculated in χ PT, a model-independent effective field theory [16], but it is not clear how high in Q^2 these calculations can be applied [17, 18]. Thus Γ_1 presents a calculable observable that spans the entire energy range from fundamental degrees of freedom (quarks and gluons) to effective ones (hadrons).

Higher moments of g_1 are interesting as well. In our kinematic domain, these moments emphasize the resonance region over DIS kinematics because of extra factors of x in the integrand. The fundamental generalized forward spin polarizability of the nucleon is given by [19]

$$\gamma_0(Q^2) = C(Q^2) \int_0^{x_0} x^2 \left\{ g_1(x, Q^2) - \frac{4M^2}{Q^2} x^2 g_2(x, Q^2) \right\} dx, \quad (2)$$

where the kinematic factor $C(Q^2) = 16\alpha M^2/Q^6$ and α is the fine structure constant. At high Q^2 one would expect g_2 to diminish significantly and g_1 to vary logarithmically with Q^2 , thus γ_0 weighted by Q^6 should be largely independent of Q^2 [1, 19, 20]. A measurement of γ_0 on the neutron indicates no evidence for such “scaling” below $Q^2 = 1$ GeV², and furthermore the data barely agree with χ PT calculations at low Q^2 [21]. No measurement of γ_0 on the proton has been reported so far.

In order to advance our theoretical understanding of the nucleon spin, it is essential to have data on the spin structure functions at low Q^2 and in the resonance region, as well as at DIS kinematics. Data in the resonance region are necessary to calculate moments, especially at low and moderate Q^2 . Until recently, data in the resonance region were quite scarce [22], but new measurements of spin structure functions in the resonance region have now been reported on proton [23, 24], deuteron [25] and ³He targets [26, 27] from Jefferson Lab. Testing χ PT at low Q^2 has increasingly been a focus of new spin structure experiments [28, 29, 30].

The EG1 experiment of the CLAS collaboration has collected new data using longitudinally polarized 1.6 and 5.7 GeV electrons on proton (NH₃) and deuteron (ND₃) targets [31]. These data cover a wide kinematic range that includes invariant mass $W^2 = M^2 + 2M\nu - Q^2$ from elastic scattering (quasielastic for the deuteron) up to 9 GeV² [32, 33]. First results for the generalized forward spin polarizability of the proton and new results for the first moments of g_1^p and g_1^d at low and intermediate Q^2 in the range $0.05 < Q^2 < 3$ GeV² are reported in this letter.

In the EG1 experiment, the beam was produced from a strained GaAs wafer and had an average polarization

of 70% as measured by Moller polarimetry [34]. The polarization of the electrons was flipped at 30 Hz pseudo-randomly. The beam was rastered over the face of the target cell to avoid heating and depolarization. The current varied from 0.3 nA to 10 nA depending on the beam conditions and target.

The product of the beam and target polarizations $P_b P_t$ was determined from the data through comparison with the known elastic scattering asymmetry and ranged from 0.50 to 0.60 for the NH₃ target and from 0.12 to 0.23 for the ND₃ target. Data were also taken with ¹²C, ⁴He and frozen ¹⁵N to determine the dilution from unpolarized materials [35].

Scattered electrons were detected in the CEBAF Large Acceptance Spectrometer (CLAS) in Hall B [34], covering a range in polar angle from 8° to 45° in the efficient region of the detector. Data acquisition was triggered by a coincidence between the Čerenkov detector and the calorimeter in any one of the six sectors. Only electrons detected in a region of the Čerenkov detector with an efficiency greater than 80% were used in the analysis. Additional details about the experiment can be found in Refs. [25, 32].

We measured the raw inclusive double spin asymmetry with longitudinally polarized beam and target in each Q^2 and W bin. This raw asymmetry was then corrected for the difference in accumulated charge in the two beam polarization states, e^+e^- pair production and pion contamination. Polarization and dilution factors were divided out and radiative corrections applied. The resulting asymmetry, $A_{//}$, is proportional to a linear combination of the two virtual photon asymmetries A_1 and A_2 [25]. Using a parameterization of the world data to model A_2 [25], the unpolarized structure function F_1 [36, 37], and the ratio of transverse to longitudinal structure functions R [36], A_1 and g_1 were extracted using:

$$A_1(x, Q^2) = \frac{1}{D} A_{//} - \eta A_2, \quad (3)$$

$$g_1(x, Q^2) = \frac{F_1}{1 + \gamma^2} (A_1 + \gamma A_2), \quad (4)$$

where the depolarization factor D depends on R , η is a kinematical factor and $\gamma^2 = \frac{Q^2}{\nu^2}$. The generalized forward spin polarizability for the proton was calculated from the data for A_1 and the F_1 parameterization using $\gamma_0(Q^2) = C \int_0^{x_0} A_1 F_1 x^2 dx$, which is equivalent to Eq. (2).

The total systematic error on g_1 varies greatly depending on the kinematic bin; for the proton it is roughly 10% and for the deuteron it is typically 15% for the 1.6 GeV data and 20% for the high energy data. The systematic error is dominated by model uncertainties on A_2 , F_1 and R , which are estimated by using different parametrizations of the world data. For the deuteron data the uncertainty in $P_b P_t$ also contributes substantially to the systematic error.

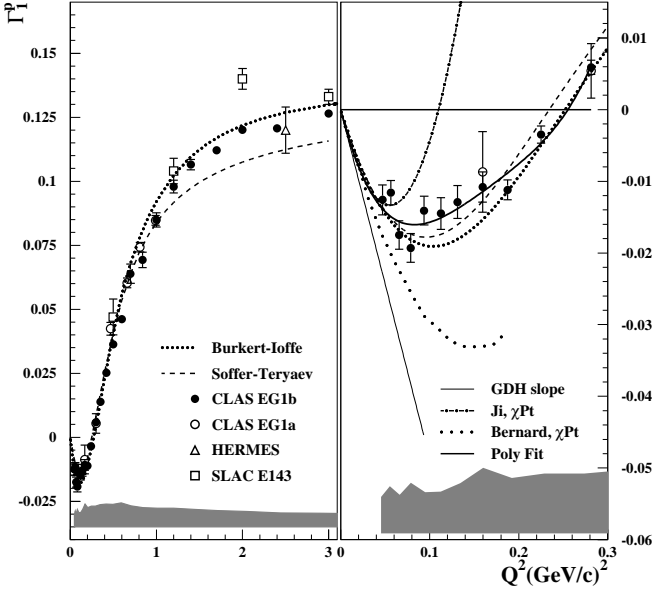


FIG. 1: Γ_1^p as a function of Q^2 . The data reported here (EG1b) are shown as the solid circles, along with the earlier EG1 data (EG1a)[23], SLAC [22] and Hermes data [9], shown for comparison. The filled circles represent the present data, including an extrapolation over the unmeasured part of the x spectrum using a model of world data. Phenomenological models of Burkert and Ioffe [39, 40] and Soffer and Teryaev [41] are represented by solid and dashed lines, respectively. The grey band represents the systematic error. In the right plot, the scales are expanded and χ PT calculations from Bernard [17] and Ji [18] are included.

The values of g_1^p and g_1^d were extracted for Q^2 from 0.05 to 5 GeV^2 and for x greater than 0.1; all results are available from the CLAS database [38]. At low Q^2 , the $\Delta(1232)$ resonance is quite prominent, with a negative asymmetry as expected for this transition. It decreases steadily in strength as Q^2 increases. In the mass region above the $\Delta(1232)$ resonance, g_1 increases from nearly zero to large positive values as Q^2 increases. In the $\Delta(1232)$ region and at low Q^2 , $g_1^d/2$ is consistent with g_1^p , as expected for a transition to an isospin $\frac{3}{2}$ state. However, at high Q^2 , g_1^p is significantly larger than $g_1^d/2$, indicating a negative contribution from the neutron.

The first moments of g_1^p and g_1^d are shown in Figs. 1 and 2, respectively. The parametrization of world data [38] is used to include the unmeasured contribution to the integral down to $x = 0.001$. The systematic uncertainty (shown by the grey bands) includes the model uncertainty from the extrapolation to the unmeasured region. Only the Q^2 bins in which the measured part (summed absolute value of the integrand) constitutes at least 50% of the total integral are shown. For the proton, the parametrization is also used at high x (in the range

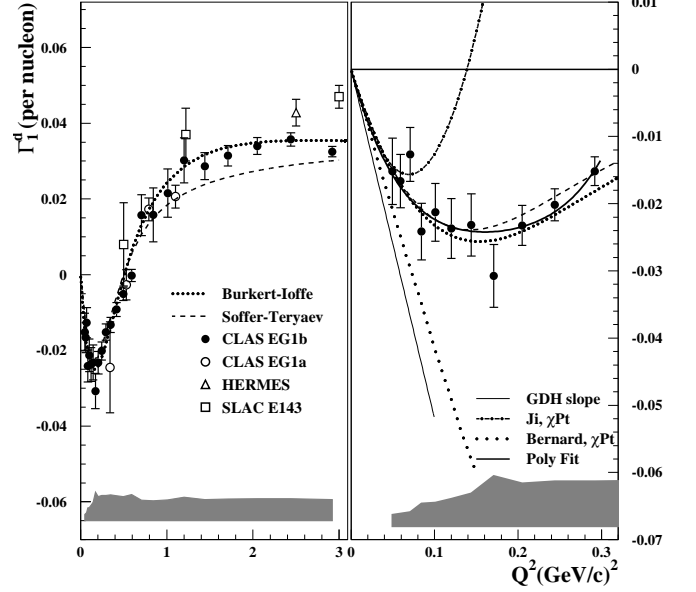


FIG. 2: Γ_1^d as a function of Q^2 . The symbols and curves are the same as for Fig. 1.

$1.09 < W < 1.14$ (1.15) GeV for the 1.6 (5.7) GeV data). For the deuteron, the integration is carried out up to the nucleon pion production threshold at high x , excluding the quasi-elastic and electro-disintegration contributions. Our low Q^2 coverage allows us to observe, for the first time, the slope changing sign at low Q^2 , consistent with the expectation of a negative slope given by the GDH sum rule at very low Q^2 . In general the data are well described by the phenomenological models of Burkert and Ioffe [39, 40] and Soffer and Teryaev [41].

The low Q^2 Γ_1 data are shown in more detail in the right-hand panels of Figs. 1 and 2. It is possible to make a quantitative comparison between our results for Γ_1^p and Γ_1^d at low Q^2 and the next-to-leading order χ PT calculation by Ji, Kao and Osborne [18], who find $\Gamma_1^p(Q^2) = -\frac{\kappa_p^2}{8M^2}Q^2 + 3.89Q^4 + \dots$ and $\Gamma_1^n(Q^2) = -\frac{\kappa_n^2}{8M^2}Q^2 + 3.15Q^4 + \dots$. Treating the deuteron as the incoherent sum of a proton and a neutron, and correcting for the D -state as discussed in Ref. [42],

$$\Gamma_1^d(Q^2) = \frac{1}{2}(1 - 1.5\omega_D) \{ \Gamma_1^p(Q^2) + \Gamma_1^n(Q^2) \}, \quad (5)$$

where $\omega_D = 0.056$ is the weight of the D -wave in the deuteron, one finds that $\Gamma_1^d(Q^2) = -0.451Q^2 + 3.26Q^4$. In the range of Q^2 from 0 to 0.3 GeV^2 , we fit Γ_1^p and Γ_1^d to a function of the form $aQ^2 + bQ^4 + cQ^6 + dQ^8$, where a is fixed at -0.456 (proton) and -0.451 (deuteron) by the GDH sum rule. Note that the GDH sum rule on the deuteron here excludes the two-body breakup part, which otherwise nearly cancels the inelastic contribution [43].

The fit results for the proton, $b = 4.31 \pm 0.31$ (stat) ± 1.36 (syst), and for the deuteron, $b = 3.19 \pm 0.44$ (stat) ± 0.68 (syst), are both consistent with the Q^4 term predicted by Ji *et al.* [18]. The fit (labelled “Poly Fit”) is shown in the right-hand panels of Figs. 1 and 2 along with Ji’s prediction. Clearly the Q^6 term becomes important even below $Q^2 = 0.1$ GeV² and this term needs to be included in the χ PT calculations in order to extend the range of their validity beyond roughly $Q^2 = 0.06$ GeV². The χ PT 4th order (one-loop), relativistic calculation by Bernard *et al.* [17] is also shown in Figs. 1 and 2. Not shown is the result from Bernard *et al.* that includes an estimate of the $\Delta(1232)$ and vector meson degrees of freedom, which are important at low Q^2 . That result has large uncertainties and is consistent with our data.

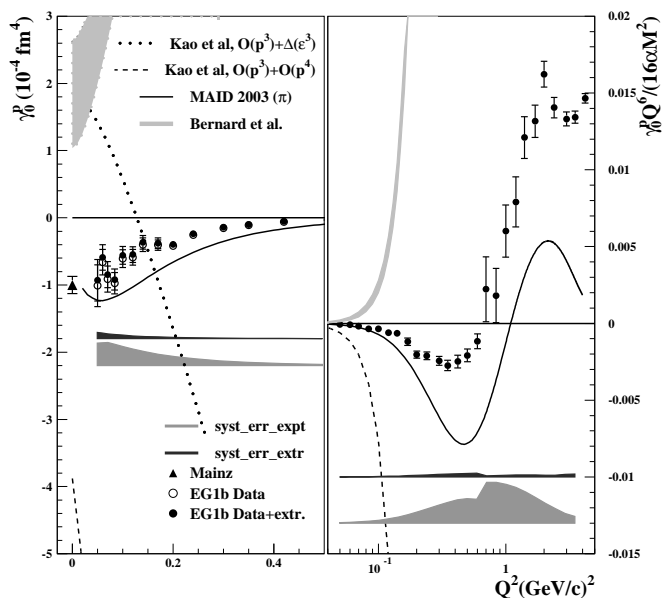


FIG. 3: Generalized forward spin polarizability γ_0^p as a function of Q^2 for the full integral (closed circles), the measured portion of the integral (open circles) and $Q^2 = 0$ [44] (triangle). The systematic error on the measured (grey) and unmeasured (dark) contributions are indicated by bands. χ PT calculations [17, 45] are shown along with MAID 2003 [46]. The data shown on the right are weighted by $Q^6/(16\alpha M^2)$.

Fig. 3 shows the result for the generalized forward spin polarizability of the proton $\gamma_0^p(Q^2)$. Since γ_0 is weighted by an additional factor of x^2 compared to Γ_1 , the integral is mostly saturated by the $\Delta(1232)$ resonance and uncertainties due to the low- x extrapolation are greatly reduced. The MAID 2003 [46] model follows the trend of the data but lies systematically below them. The MAID model is consistent with our data for A_1 in the Δ resonance region, but MAID includes only single-pion production channels, which leads to an underestimation of the unpolarized structure function F_1 entering the definition

of γ_0 .

Unlike Γ_1 , γ_0 is not constrained at $Q^2 = 0$ and is therefore a more stringent test of Chiral Perturbation calculations. The leading order heavy baryon χ PT calculation by Kao, Spitzenberg and Vanderhaeghen [45], shown by the dotted line in Fig. 3, includes the Δ resonance contribution. Their 4th order calculation (dashed line) is of opposite sign and shows no sign of convergence; neither calculation reproduces the trend or magnitude of the data. The relativistic χ PT calculation of Bernard, Hemmert and Meissner converges better at 4th order [17]. That calculation, including the resonance contribution, is represented by the grey band in Fig. 3, and is also in serious disagreement with the data. The $\Delta(1232)$ and vector meson contribution is negative (around -2×10^{-4} fm⁴) and is consistent with the calculation by Kao *et al.* at $Q^2 = 0$, suggesting that the discrepancy at low Q^2 is mainly due to the non-resonance terms [47].

In the right-hand panel of Fig. 3, γ_0^p is weighted by a factor of $Q^6/(16\alpha M^2)$. For Q^2 above 1.5 GeV², the data seem to plateau, although it is not possible to verify the trend without data at higher Q^2 . At very high Q^2 , the Q^6 -weighted γ_0 converges to the 2nd moment of g_1 , a_2 , which is expected to scale in the framework of OPE.

In summary, $g_1(x, Q^2)$ for the proton and the deuteron have been measured over a vastly expanded kinematic range at low and intermediate momentum transfer, which includes the entire resonance region and part of the DIS regime. These measurements enable us to evaluate moments of g_1 over a wider range in Q^2 , decreasing extrapolation uncertainties. The first measurement of γ_0^p has been reported along with a new precise mapping of Γ_1^p and Γ_1^d down to lower Q^2 than previously available. At high Q^2 we observe that $Q^6\gamma_0^p$ levels off and we see the expected trend toward DIS results in Γ_1 . It will be interesting to extend these measurements to higher Q^2 once the upgraded beam energy is available at Jefferson Lab. At low Q^2 , the first moments of g_1^p and g_1^d exhibit a change in the sign of the slope, to match the negative slope constraint from the generalized GDH sum rule, and are consistent with χ PT calculations for momentum transfer values up to about 0.06 GeV². It is important to note, however, that these χ PT calculations also assume the validity of the GDH sum rule; a more sensitive test of χ PT calculations is $\gamma_0(Q^2)$. We observe that χ PT calculations fail to describe our results for γ_0^p , even for Q^2 as low as 0.05 GeV². The χ PT calculations are increasingly being used to extract results from lattice QCD and it is critical to understand their range of applicability [16]. Data for the isoscalar quantity $\gamma_0^p - \gamma_0^n$ have also been published by our collaboration and may give additional guidance to future theoretical work in this area [48]. We also look forward to results from new experiments at Jefferson Lab, in which spin structure functions down to $Q^2 = 0.01$ GeV² will provide a more stringent test of χ PT [28, 29, 30].

We would like to acknowledge the outstanding efforts of the staff of the Accelerator and the Physics Divisions at Jefferson Lab that made this experiment possible. This work was supported in part by the U.S. Department of Energy and National Science Foundation, the Italian Istituto Nazionale di Fisica Nucleare, the French Centre National de la Recherche Scientifique, the French Commissariat à l’Energie Atomique and the Korean Science and Engineering Foundation. Jefferson Science Associates operates the Thomas Jefferson National Accelerator Facility for the United States Department of Energy under contract DE-AC05-84ER-40150. We would also like to thank M. Vanderhaeghen for helpful discussions.

* Contact Author gdodge@odu.edu

† deceased

- [1] J.-P. Chen et al., *Mod. Phys. Lett.* **A20**, 2745 (2005).
- [2] S. B. Gerasimov, *Sov. J. Nucl. Phys.* **2**, 430 (1966).
- [3] S. Drell and A. Hearn, *Phys. Rev. Lett.* **16**, 908 (1966).
- [4] K. Abe et al., *Phys. Rev.* **D58**, 112003 (1998).
- [5] P. L. Anthony et al., *Phys. Lett.* **B493**, 19 (2000).
- [6] B. Adeva et al., *Phys. Lett.* **B412**, 414 (1997).
- [7] D. Adams et al., *Phys. Lett.* **B396**, 338 (1997).
- [8] V. Alexakhin et al., *Phys. Lett.* **B647**, 8 (2007).
- [9] A. Airapetian et al., *Phys. Rev.* **D75**, 012007 (2007).
- [10] X. Ji and J. Osborne, *J. Phys. G* **27**, 127 (2001).
- [11] A. Deur et al., *Phys. Rev. Lett.* **93**, 212001 (2004).
- [12] Z. E. Meziani et al., *Phys. Lett.* **B613**, 148 (2005).
- [13] M. Osipenko et al., *Phys. Lett.* **B609**, 259 (2005).
- [14] S. Simula et al., *Phys. Rev.* **D65**, 034017 (2002).
- [15] M. Osipenko et al., *Phys. Rev.* **D71**, 054007 (2005).
- [16] V. Bernard *Prog. Part. Nucl. Phys.* **60**, 82 (2008).
- [17] V. Bernard et al., *Phys. Rev.* **D67**, 076008 (2003).
- [18] X. Ji et al., *Phys. Lett. B* **472**, 1 (2000).
- [19] D. Drechsel et al., *Phys. Rept.* **378**, 99 (2003).
- [20] D. Drechsel and L. Tiator, *Ann. Rev. Nucl. Part. Sci.* **54**, 69 (2004), [nucl-th/0406059](#).
- [21] M. Amarian et al., *Phys. Rev. Lett.* **93**, 152301 (2004).
- [22] K. Abe et al., *Phys. Rev. Lett.* **78**, 815 (1997).
- [23] R. Fatemi et al., *Phys. Rev. Lett.* **91**, 222002 (2003).
- [24] F. Wesselmann et al., *Phys. Rev. Lett.* **98**, 132003 (2007).
- [25] J. Yun et al., *Phys. Rev.* **C67**, 055204 (2003).
- [26] M. Amarian et al., *Phys. Rev. Lett.* **89**, 242301 (2002).
- [27] M. Amarian et al., *Phys. Rev. Lett.* **92**, 022301 (2004).
- [28] M. Ripani, M. Battaglieri, A. Deur, and R. De Vita (2003), Jefferson Lab experiment E-03-006.
- [29] A. Deur, G. Dodge, and K. Slifer (2006), Jefferson Lab experiment E-06-017.
- [30] J.-P. Chen, A. Deur, and F. Garibaldi (1997), Jefferson Lab experiment E-97-110.
- [31] C. D. Keith et al., *Nucl. Instrum. Meth.* **A501**, 327 (2003).
- [32] K. Dharmawardane et al., *Phys. Lett.* **B641**, 11 (2006).
- [33] P. Bosted et al., *Phys. Rev.* **C75**, 035203 (2007).
- [34] B. A. Mecking et al., *Nucl. Instrum. Methods Phys. Res., Sect. A* **503**, 513 (2003).
- [35] P. Bosted et al., *Phys. Rev.* **C78**, 015202 (2008).
- [36] E. Christy and P. Bosted, (2007), [arXiv:0712:3731 \[hep-ph\]](#).
- [37] E. Christy and P. Bosted, *Phys. Rev.* **C77**, 065206 (2008).
- [38] URL <http://clasweb.jlab.org/physicsdb/>.
- [39] V. D. Burkert and B. L. Ioffe, *Phys. Lett.* **B296**, 223 (1992).
- [40] V. D. Burkert and B. L. Ioffe, *J. Exp. Theor. Phys.* **78**, 619 (1994).
- [41] J. Soffer and O. Teryaev, *Phys. Rev.* **D70**, 116004 (2004).
- [42] C. Ciofi degli Atti, L. P. Kaptari, S. Scopetta, and A. Y. Umnikov, *Phys. Lett.* **B376**, 309 (1996).
- [43] H. Arenhövel et al., *Phys. Rev. Lett.* **93**, 202301 (2004).
- [44] H. Dutz et al., *Phys. Rev. Lett.* **91**, 192001 (2003).
- [45] C. Kao et al., *Phys. Rev.* **D67**, 016001 (2003).
- [46] D. Drechsel, S. Kamalov, and L. Tiator, *Nucl. Phys.* **A645**, 145 (1999).
- [47] M. Vanderhaeghen, private communication.
- [48] A. Deur et al. *Phys. Rev. D* **78**, 032001 (2008).